Study by numerical simulations on the breathing effect in a semi-underground highway with beams and a roof above it

M Hagiwara
East Nippon Expressway Co., Ltd, Japan

A Mizuno, T Tsutaki
Kogakuin University, Japan

K Takahashi
FITUT Laboratory Co., Ltd, Japan

ABSTRACT

In the semi-underground portions there is an exchange of air through the gaps of the structure over them caused by the traffic and natural wind. This breathing phenomenon has been studied and estimated so far, but they don't refer to the influence of the structure over expressways on the breathing.

We adapt the 3D numerical simulations with the traffic included in it to a certain semi-underground road with a complex overhead structure such as beams and roofs in order to estimate their influence on the breathing. In this paper we present some of the results and then discuss them.

NOMENCLATURE

A_r	cross sectional area of the road	m^2
A_s	cross sectional area of the opening over semi-underground road	m^2
g_e	unit emission volume of CO out of the traffic	m^3/s.m
c_{r1}	concentration of CO from the tunnel upstream	-
c_{r2}	concentration of CO to the tunnel downstream	-
c_s	concentration of CO on the semi-underground road	-
H_1	height of the tunnel	m
H_2	height of the overhang	m
K	width ratio of w to W	-
l_r	length of a road in the numerical domain	m
Q_{r1}	flow from the tunnel upstream	m^3/s
Q_{r2}	flow to the tunnel downstream	m^3/s
Q_s	breathing value	m^3/s
$q*$	non-dimensional breathing value ($q*=Q_s/V_r A_s$)	-
V_{r1}	airflow velocity from the tunnel upstream	m/s
W	width of the road	m
w	width of the opening over semi-underground road	m

1 INTRODUCTION

As seen in Fig. 1 in the semi-underground portions on expressways there is an exchange of air through the gaps of the structure over the road caused by the movement of vehicles, longitudinal air flow, exterior natural wind and so on. This is called the breathing phenomenon and has been studied and estimated so far both by various experiments and numerical analyses. (1)(2)(3)

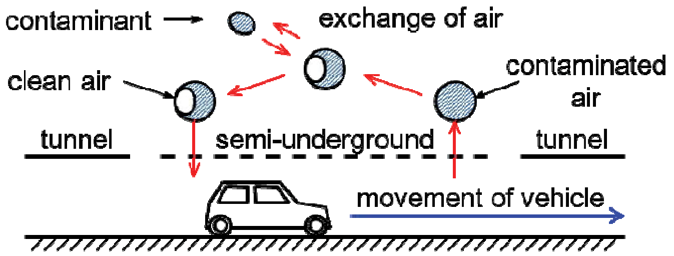

Fig. 1 schematic outline of breathing effect

However, roofs are required lately in addition to beams over the semi-underground road to prevent rainwater from dropping on the surface of the road and/or to prevent direct sunlight from coming to the road. The former increases the drainage cost and the latter annoys drivers by the flickering sunlight through the beams.

For the semi-underground road with such a complex structure in it as mentioned above, the breathing phenomena have been studied and evaluated individually (4), but there is no general way of studying.

We adapt the 3D numerical simulations with the traffic included in it to a certain semi-underground expressway with a complex overhead structure such as beams and a roof in order to evaluate their effects on the breathing. In this paper we present some of the results, make some comparisons with conventional methods and then discuss them.

2 STUDIED STRUCTURE

Fig. 2 shows the structure of the semi-underground expressway studied, but without the roof for illustrative purposes:

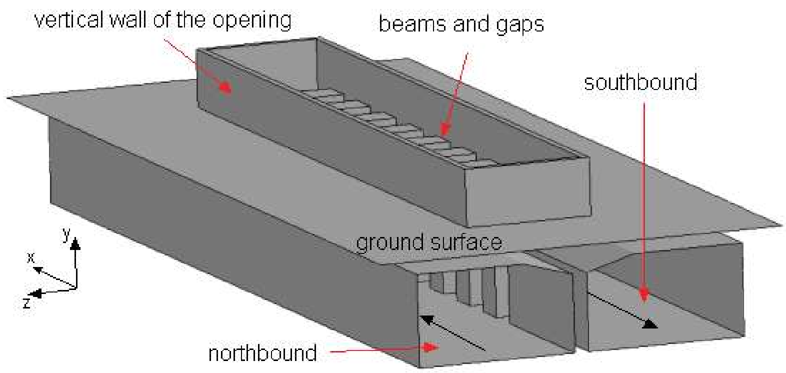

Fig. 2 Studied structure without the roof

There are two parallel roads, named northbound and southbound for two-way traffic with a common opening up above across them. The opening is surrounded by vertical walls, so the actual level of the opening is higher than the ground level.

Fig. 3 shows the interior structure. The pillars with beams at a constant interval separate the two roads, so the gaps between two pillars directly connect the two roads for the air. A plain roof is set above the vertical walls with some gap between them.

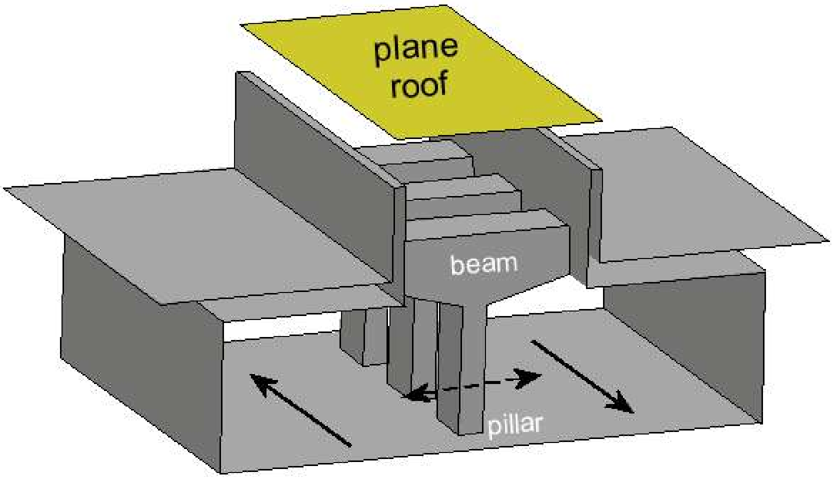

Fig. 3 Interior structure with a plain roof

In the structure mentioned above, these are factors that affect the breathing effect:

1) length of each gap between two pillars and beams
2) The existence of the roof
3) Total longitudinal airflow with two-way traffic taken into account

3 STUDY OF THE BREATHING EFFICIENCY BY 3D NUMERICAL SIMULATIONS

There has been a conventional method (5) to calculate the breathing effect of the semi-underground road. In this method, however, we cannot set the specifications of beams, pillars or a roof in its equation as will be seen in section 6.3. Moreover, the method says neither the length of the semi-underground road nor its traffic conditions have anything to do with the breathing efficiency.

We don't think its story is correct. That is why we made this study.

The software we took this time for the 3D numerical simulations is STAR-CD with "the sliding mesh" in it to express the movement of vehicles. This combining technology was developed by the Kogakuin University to study phenomena regarding various tunnel ventilation issues along with traffic. Actually, a simple semi-underground expressway was once studied by this method (3).

Fig. 4 shows the analysed area by simulations. The area includes a certain semi-underground portion and tunnel portions on both sides of it. In the simulations the downstream edge and the upstream edge of the area are connected by the cyclic boundary conditions. So, both the longitudinal airflow and the contaminants virtually circulate the area along with vehicles.

The advantages of this way of thinking will be explained later in this paper.

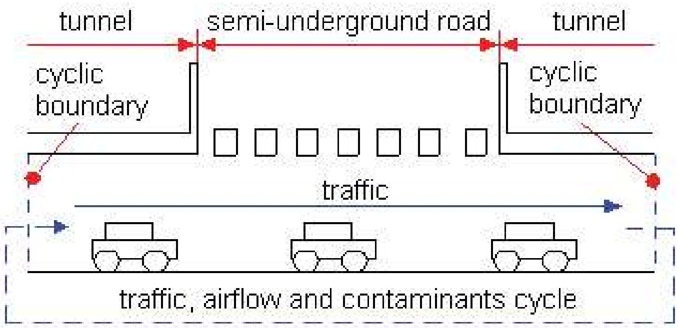

Fig. 4 Analysed area

4 CASES TO BE STUDIED

The total number of simulations we made was 12. In those simulation cases suffix A after each case name means simulations without the roof and B means with the roof.

Cases with suffix A were made basically for the comparison with cases with suffix B to make sure the influence of the roof. In addition to that, however, in the simulations with suffix A, we treated following ones as variables:

・traffic conditions
・the length of the semi-underground road
・the height of overhang (see Fig. 5 and Fig. 6)

Cases with suffix A are listed in Table 1.

Table 1 Simulation cases with suffix A (without the roof)

	Traffic	Length of the semi-underground road	Height of the overhang
Case A-a1	Normal	52.5 m	10 m
Case A-a2	Normal	102.5 m	5 m
Case A-a3	Normal	202.5 m	5 m
Case A-b1	Congestion	52.5 m	10 m
Case A-b2	Congestion	102.5 m	5 m
Case A-b3	Congestion	202.5 m	5 m

Meanwhile, cases with suffix B were simulated to evaluate the effect of the space between the roof and the top of the overhang. We adopted 2 m and 3 m for the gaps between the roof and the top of the overhang. Cases with suffix B are listed in Table 2.

.

Table 2 Simulation cases with suffix B (with the roof)

	Traffic	Length of the semi-underground road	Height of the overhang	Space between the roof and the top of overhang
Case B-a1	Normal	52.5 m	5 m	2 m
Case B-a2	Normal	52.5 m	5 m	3 m
Case B-a3	Normal	52.5 m	10 m	2 m
Case B-a4	Normal	52.5 m	10 m	3 m
Case B-b1	Congestion	52.5 m	5 m	2 m
Case B-b2	Congestion	52.5 m	5 m	3 m

3D simulation cases listed in Table 1 and Table 2 were made under following conditions:

4.1 Structure and area for the simulations

Drawings in Fig. 5 and Fig. 6 show the longitudinal view and sectional view of the semi-underground road and tunnels on both sides. These areas are included in the region for the numerical analyses. The drawings in Fig. 5 and Fig. 6 show the location of each variable. As seen in these drawings, three kinds of the semi-underground road length and two kinds of the height of overhang come to four kinds of the area to be simulated, while Fig. 7 shows what the roof is like.

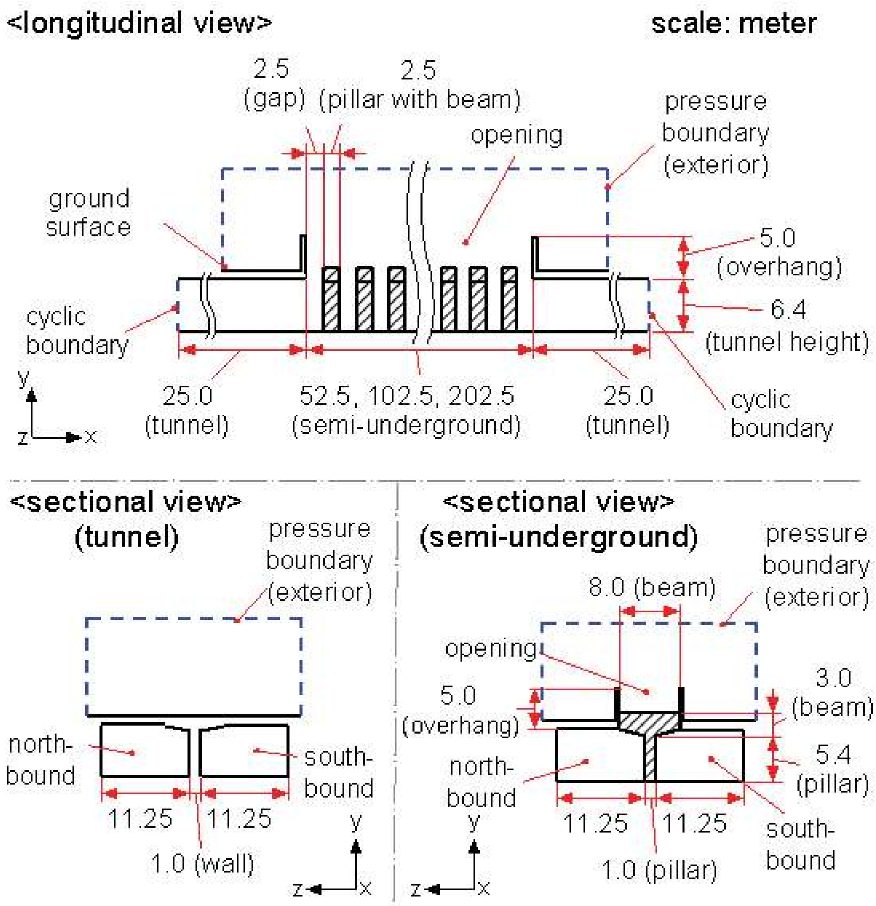

Fig. 5 The simulation area (height of the overhang: 5 m)

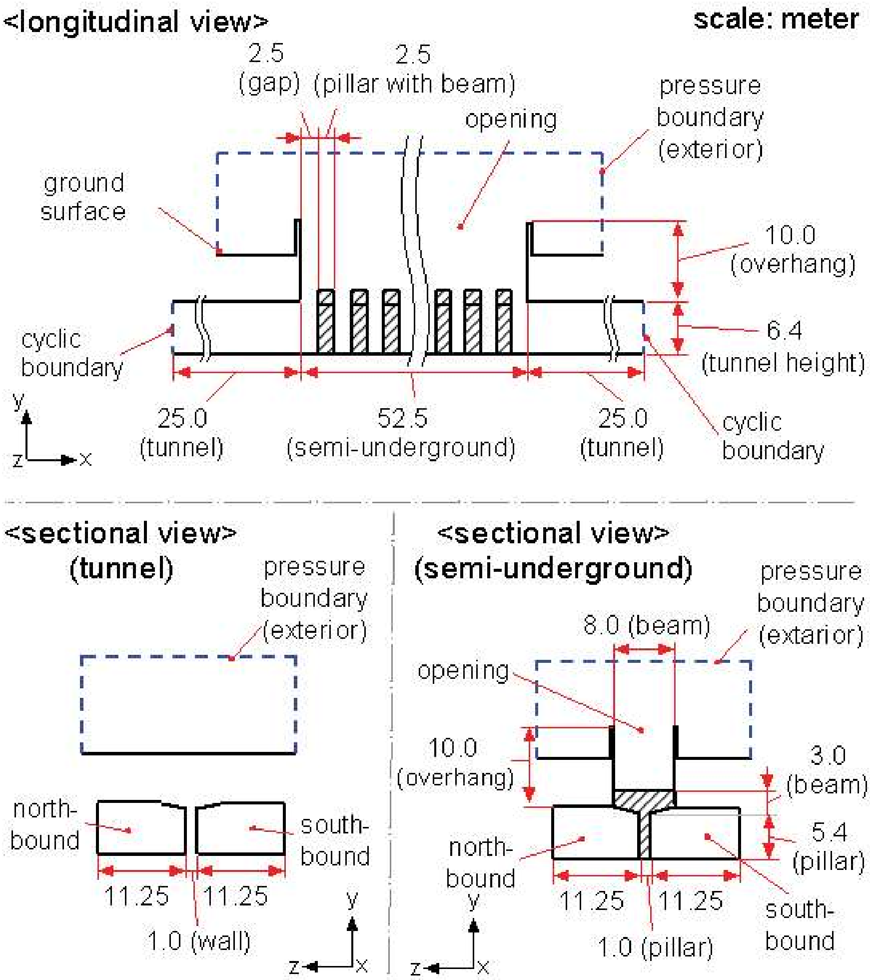

Fig. 6 The simulation area (height of the overhang: 10 m)

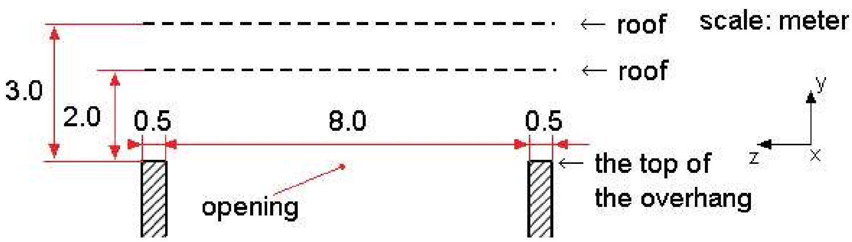

Fig. 7 Roof and its locations

The width of pillars themselves and the distance between the pillars are always constant (=2.5 m), so the number of the pillars changes following the length of the semi-underground road. The thickness of the roof was regarded as zero and its supports were ignored in the simulations.

4.2 Traffic conditions for the simulations

Two kinds of traffic conditions were taken for the simulations. They are summarized in Table 3.

We set carbon monoxide (CO) as the subject contaminant in simulations although any contaminant can be chosen to evaluate the breathing effect. The main reason is that its emission is scarcely influenced by road gradient, velocity of vehicles and so on.

Table 3 List of the traffic conditions

	Amount of traffic each bound	Velocity	L.V.R	Amount of exhausted CO /m
Normal	2816 veh/h	60 km/h	0.33	3.876×10^{-6} m^3/s m
Congestion	3224 veh/h	18 km/h	0.33	5.833×10^{-6} m^3/s m

Using the traffic conditions in Table 3, we made vehicles run on the two lanes of each bound in a zigzag disposition as shown in Fig. 8 (a).

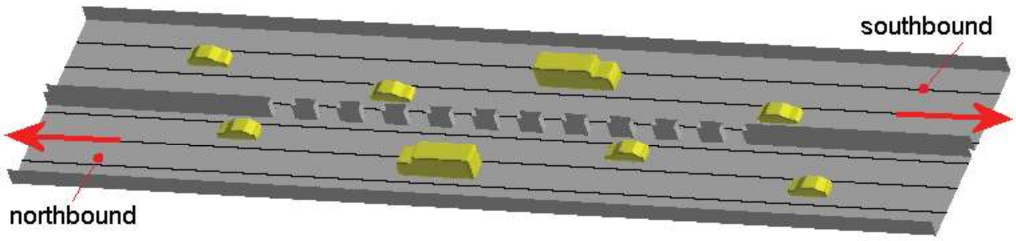

(a) Movement of vehicles in the simulation area (normal traffic)

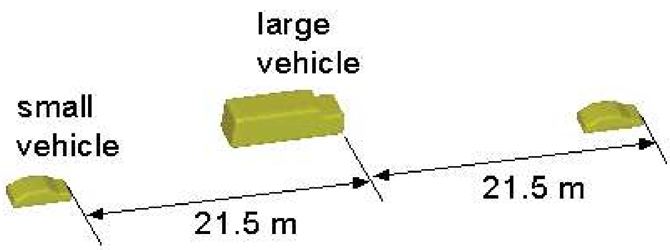

(b) Layout of vehicles on one road in normal traffic

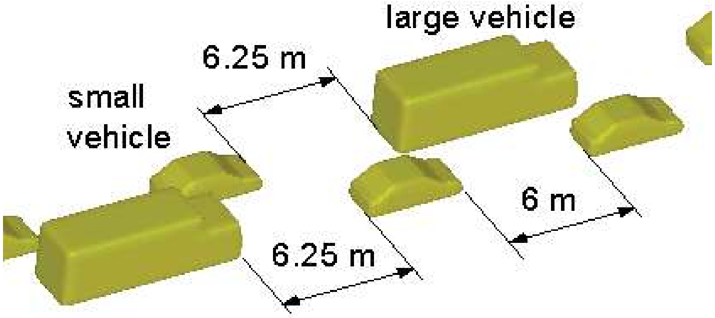

(c) Layout of vehicles on one road in congestion

Fig. 8 Layout of vehicles in simulations

4.3 Conditions of the ventilation for the simulations

In the simulations neither mechanical ventilation nor natural wind was included, so only the movement of vehicles causes the airflow in the simulation area. Each simulation consists of two steps:

The first step: keeping the vehicles running in a simulation until the airflow distribution in the total area reaches equilibrium.

The second step: when the first step is over, letting the simulation to analyse the behaviour of the contaminant from vehicles start.

5 RESULTS OF THE SIMULATIONS

Table 4 shows the results of two factors from the simulations: one is hourly averages of the longitudinal airflows in the tunnel portion (Q_{r1})), and the other is CO concentrations under beam level in a semi-underground road averaged by both time and space (c_s).

Using these outputs, we calculated the breathing efficiency in the semi-underground road portion.

Table 4 Results from 3D simulations

	Q_{r1}	c_s
Case A-a1	507.2 m^3/s	23.0 ppm
Case A-a2	514.5 m^3/s	18.6 ppm
Case A-a3	513.0 m^3/s	14.2 ppm
Case A-b1	187.0 m^3/s	44.9 ppm
Case A-b2	188.0 m^3/s	36.6 ppm
Case A-b3	188.2 m^3/s	31.3 ppm

	Q_{r1}	c_s
Case B-a1	501.8 m^3/s	33.0 ppm
Case B-a2	501.8 m^3/s	29.1 ppm
Case B-a3	502.3 m^3/s	34.7 ppm
Case B-b4	502.4 m^3/s	29.1 ppm
Case B-b1	182.5 m^3/s	96.9 ppm
Case B-b2	182.8 m^3/s	82.1 ppm

6 EVALUATION OF BREATHING EFFECT BASED ON THE SIMULATIONS

In this chapter we talk about evaluation of breathing effect based on the simulations.

6.1 Values used for the evaluation of the breathing effect

Fig. 9 explains a concept of Q_s, which corresponds to the total amount of the air with contaminants in it that is exhausted to the exterior space per second through an opening with the cross sectional area of A_s when the velocity of longitudinal airflow is V_r. Q_s is called the breathing value and is one of the key to evaluating the breathing effect.

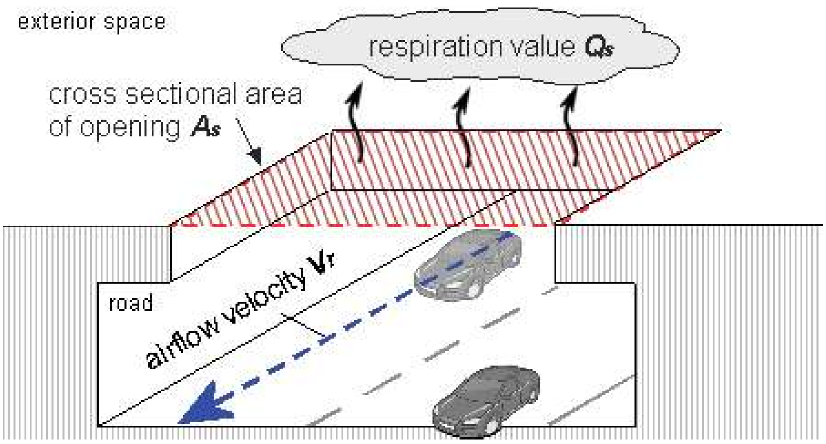

Fig. 9 Conception of the breathing value: Q_s

However, when we compare one breathing effect with others in different settings, using just the breathing value is not appropriate because it varies considerably depending on the sectional area of the opening and airflow velocity around the road. In order to eliminate influences from these factors, the non-dimensional breathing value ($q*$) is usually adopted:

$$q* = Q_s / A_s \cdot V_r \quad (1)$$

We also conducted our study of the evaluation making use of the value $q*$.

6.2 Calculation of non-dimensional breathing value based on the 3D analysis

Now, we calculate the non-dimensional breathing values from the obtained results of the simulations listed in Table 4.

Fig. 10 diagrammatically shows how a contaminant comes into or out of the one directional road with two lanes. The calculation of the non-dimensional breathing value has been made based on the conservation law of the contaminant flow rate, which we also followed in this paper.

Since each of two roads in the opposite direction of traffic has the symmetrical geometry and the same traffic amount, amount of the contaminant exchanged between them through gaps between pillars can be ignored.

In the semi-underground road in this paper the opening occupies the space over the two roads, so we can think that a half of the breathing value ($Q_s/2$) is generated through a half of the opening ($A_s/2$) for each one of the two roads.

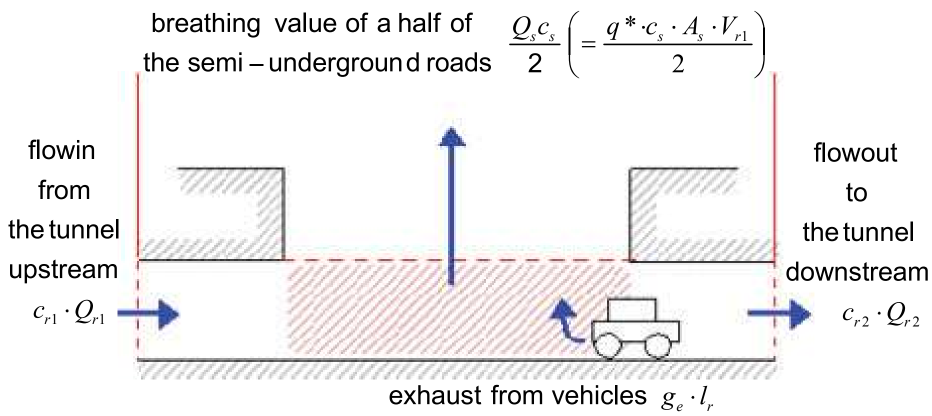

Fig. 10 Coming in and out of a contaminant for each road through the opening

In the context mentioned above the following equation can make sense based on the conservation law of the contaminant flow rate:

$$c_{r1}Q_{r1} + g_e l_r = c_{r2}Q_{r2} + \frac{q^* \cdot c_s \cdot A_s \cdot V_r}{2} \tag{2}$$

Since downstream and upstream are connected with each other by the cyclic boundary in this study, these two relations are right: $Q_{r1} = Q_{r2}$ and $c_{r1} = c_{r2}$.

So, the equation (2) comes to:

$$g_e l_r = \frac{q^* \cdot c_s \cdot A_s \cdot V_r}{2} \tag{3}$$

When you put $V_{r1} = Q_{r1} / A_{r1}$ into the equation (3), it comes to the following:

$$q^* = \frac{2g_e \cdot l_r \cdot A_r}{c_s \cdot A_s \cdot Q_1} \quad (4)$$

Putting Q_{r1} and c_s that were obtained by the 3D simulations and listed in Table 4 into equation (4), you can obtain a non-dimensional breathing value for each simulation case as listed in Table 5.

Table 5 Non-dimensional breathing value based on 3D simulations

	q*
Case A-a1	0.022
Case A-a2	0.020
Case A-a3	0.023
Case A-b1	0.045
Case A-b2	0.043
Case A-b3	0.043

	q*
Case B-a1	0.015
Case B-a2	0.017
Case B-a3	0.015
Case B-b4	0.017
Case B-b1	0.021
Case B-b2	0.025

6.3 Non-dimensional breathing value based on the conventional method

The conventional method says the non-dimensional breathing value of a semi-underground road is given by the following equation (5):

$$q^* = \frac{0.0325}{\sqrt{K}} \cdot \left(\frac{H_1}{H1 + K \cdot H_2} \right) \qquad K = \frac{w}{W} \quad (5)$$

This equation means that the non-dimensional breathing value only depends on the cross section of the semi-underground road and that it has nothing to do with its length or the traffic conditions in it. Beams and pillars also are not included in the equation (5), much less the roof is.

We applied the equation (5) to a semi-underground road with the same cross section as the one in this paper. Table 6 shows the parameters we put into equation (5) (see Fig. 5 and Fig. 6).

Table 6 Parameters for the conventional calculation

Width of the opening: *w*	8 m
Width of the road: *W*	23.5 m
Ratio of widths: *K*	0.340
Height of the tunnel: H_1	6.4 m
Height of the overhang: H_2	5 m , 10 m

Table 7 shows the results of the calculation applying parameters in Table 6 to the equation (5).

Table 7 Non-dimensional breathing value by the conventional method

H_1	***q****
H_1=5m	0.044
H_1=10m	0.036

7 CONSIDERATIONS

7.1 Influence of the overhang and the traffic conditions on the non-dimensional breathing value

In Fig. 11 results of the non-dimensional breathing values from 3D simulations without the roof (cases with suffix A) are plotted as the function of the semi-underground road length. From Fig. 11 we can say that for the semi-underground road with the structure shown in Fig. 5 and Fig. 6 the non-dimensional breathing value only depends on the traffic condition, regardless of the height of the overhang or the length of the semi-underground road.

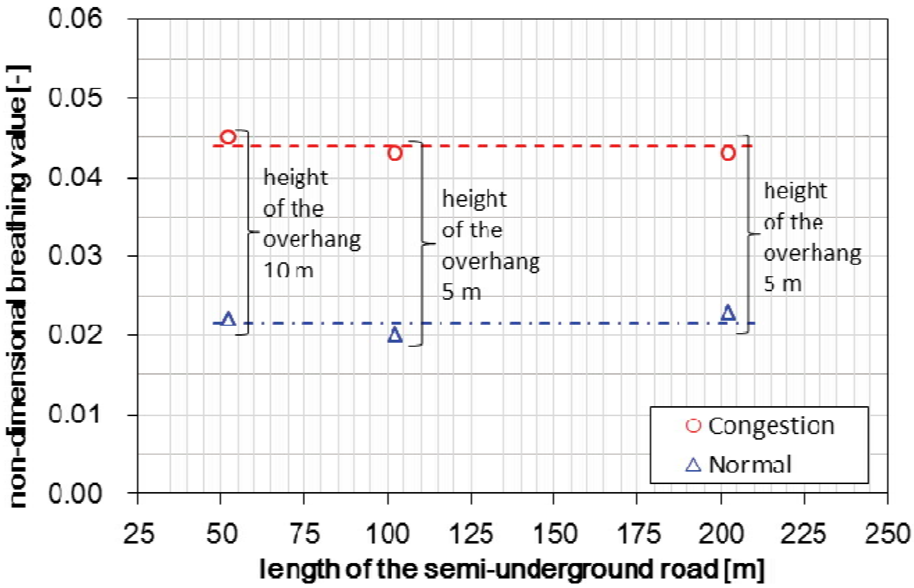

Fig. 11 Non-dimensional breathing values as the function of semi-underground road length

In the meantime, results from the conventional method insist that the non-dimensional breathing value only depends on the height of the overhang (see Table 7), regardless of the traffic conditions or the length of the road.

Results from the two different methods are completely different except that the non-dimensional breathing value is independent of the semi-underground road length.

We think that the difference between the two methods comes from the fact that the conventional method deal with the non-dimensional breathing as a 2D phenomenon. The results from 3D simulations, however, show the phenomenon is entirely three dimensional.

Fig. 12 shows a contour of the airflow velocity distribution at a given moment, which is acquired from one of the simulations. According to Fig. 12, although there is comparatively strong airflow around the traffic, there is almost no airflow in the space over the beams. Without these beams, air in the open space would be involved in the airflow around the traffic to make breathing happen between open space and semi-underground road as the past study (3) say.

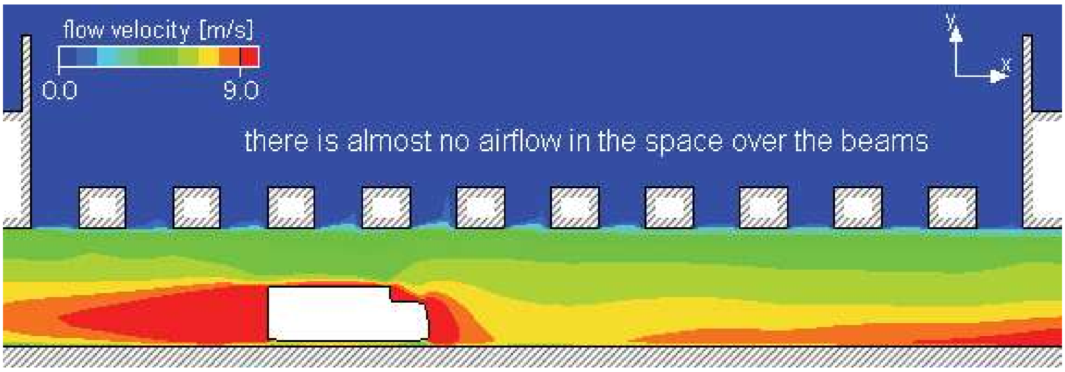

Fig. 12 Contour of airflow velocity around the traffic and open space

Fig. 13 shows velocity vectors of airflow and the concentration of CO at the same moment as Fig. 12. You can see that the longitudinal airflow around the traffic is limited to the downside of the beams and that breathing through gaps between beams is considerably small.

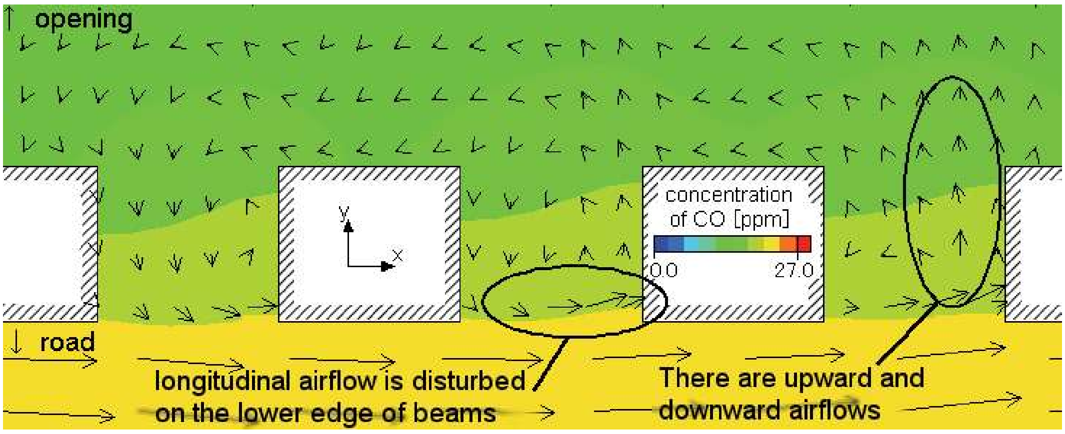

Fig. 13 Airflow vectors and concentration of CO around beams

From Fig. 12 and Fig. 13 we think that the height of the overhang does not affect the non-dimensional breathing value because the beams block the breathing and that under normal traffic the non-dimensional breathing value is smaller because the higher longitudinal airflow downside of beams also blocks the breathing through gaps. This is why we obtained the result of simulations shown in Fig. 11.

7.2 Influence of the additional roof on the non-dimensional breathing value

Fig. 14 shows the influence of the additional roof on the non-dimensional breathing value. The value with no roof for normal traffic condition comes from the average of Case A-a1, Case A-a2 and Case A-a3, and for congestion of traffic comes from the average of Case A-b1, Case A-b2 and Case A-b3 (see Table 5).

According to Fig. 14, when the distance between the roof and the top of overhang decreases, non-dimensional breathing value also decreases but the decreasing rate depends on the traffic conditions.

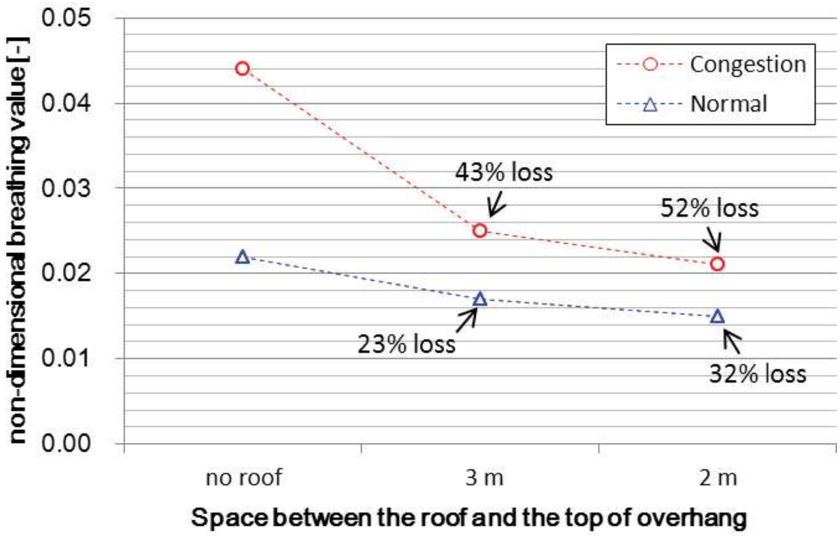

Fig. 14 Space between the roof and the top of overhang and non-dimensional breathing value (see Fig. 3 and Fig. 7)

Fig. 15 shows velocity vectors of airflow upside of beams when traffic is normal and in congestion.

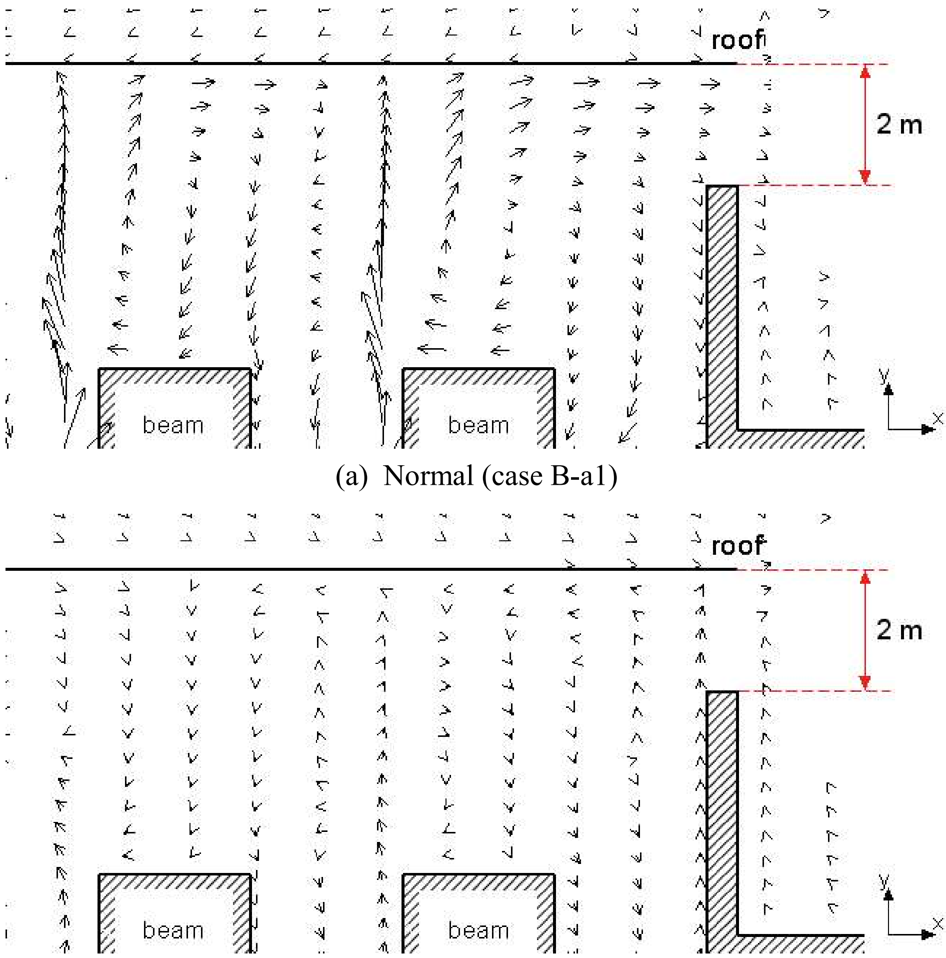

(b) Congestion (case B-b1)

Fig. 15 Velocity vectors when traffic is normal and in congestion

According to Fig. 15 (a), when the traffic is normal, airflow velocity is higher. So, the air that collides with the roof goes along the roof out to the exterior space, while there is no outstanding airflow to go to the exterior space when the traffic is in congestion (Fig. 15 (b)).

In the congestion of traffic the diffusion is dominant compared to the advection as Fig. 15 shows. The amount of diffusion is more related to the dimension of space between the roof and the top of overhang. This is why the decreasing rate of non-dimensional breathing value is larger when the traffic is in congestion as seen in Fig. 14.

8 CONCLUSIONS

Using 3D numerical analysis with "the sliding mesh" in it to express the movement of vehicles, we made a study on the influence of a complicated structured semi-underground road on its breathing effect. These are the conclusions:

- In such a complicated structured semi-underground road as the one we studied in this paper the non-dimensional breathing value does not vary as the function of the height of overhang but considerably depends on the traffic conditions. This is a new knowledge acquired. In addition to that, when the traffic is normal, discrepancy in the non-dimensional breathing value between by the conventional method and by the one in this paper gets significantly larger.
- When a roof exists above beams, it turned out that the non-dimensional breathing value depends on the distance between the roof and the top of overhang, and also appreciably depends on the traffic conditions.

As mentioned in this paper, when it comes to a semi-underground road with complicated structures, the conventional method does not work. The phenomena are so three dimensional that we need to apply 3D simulations to it.

REFERENCES

(1) H. Ohashi, T. Koso, M. Ishizuka, T. Kawada: Turbulent Mass Diffusion Through the Side Opening of Circular Pipe, Transactions of the Japan Society of Mechanical Engineers. B Vol.53, No.491, pp. 2000-2006, 1987 (in Japanese)

(2) H. Hoshino, Y. Ohta, Y. Yuasa: A Study of Natural Ventilation in Road Tunnels in Urban Areas, Fourth International Symposium on the Aerodynamics and Ventilation of Vehicle Tunnels, BHRGroup, pp261-278, York, England, March 23-25, 1982

(3) K. Yamada, Y. Hirano, A. Mizuno: Numerical Analysis of Exhaust Gas Diffusion in a Depressed Road with Consideration of Moving Vehicle, JSME annual meeting 2007(2), pp.283-284, 2007 (in Japanese)

(4) Y. Ota, R. Stroeks, Y. Sakata, N. Goto: Multi-functional louvers at half-covered roads and intermittent tunnels in urban areas: Performance and Characteristics, 14th IRF Road World Congress, 2001

(5) Highway enviromnment research institute: Technical methology of evaluation on environmental influences by roads, pp58, 2000 (in Japanese)